[1]R. Deepalaxmi

[2]C. Vaithilingam

Microcontroller Based Condition Monitoring System for Induction Motor

Journal of Electrical Systems

Abstract: Single phase motors are widely used because of their reliability, high efficiency low cost and good self-starting capability. These motors experience several types of electrical faults like over load, over/under voltages. Due to these faults, the windings of the motor get overheated which leads to insulation failure and reduces the lifetime of motor. This research proposed a control and condition monitoring protection scheme for induction motors using microcontroller Arduino UNO, bluetooth module HC-05 and various sensors.

Keywords: Condition Monitoring, Micro-controller, Induction motor, Speed sensor, Current sensor, Temperature sensor, Bluetooth module.

I. INTRODUCTION

Induction motors are electro-mechanical devices used in industries to convert electrical energy to mechanical energy. They are regarded as the workhorse of industry. These motors are used in pumps, conveyors, machine tools, presses and packaging equipment. The major advantages of these motors are that they are highly reliable, require low maintenance, and have relatively high efficiency. Induction motors are susceptible to many types of faults in industrial applications due to their continuous operation, improper supply and their operation in hazardous environments.

A fault that is not detected at an early stage may become catastrophic. Similarly induction motor may suffer from severe damage when faults are left undetected. The severe damages may cause production shutdowns. Such shutdowns are costly, in terms of production time, maintenance cost and wasted raw materials. Monitoring, protection and failure detection improves the reliability and availability of the existing system. Since the various faults degrade relatively slowly, there is a potential for fault detection at an early stage. This avoids sudden and total failures which have serious consequences. This information can be used to minimize downtime and to schedule adequate maintenance action [1]. The main objectives of this research work are implementation of closed loop control of 1-phase induction motor using PID controller and microcontroller subsystem in Matlab-simulink for variable source and variable load. The development of prototype of the condition monitoring protection scheme of single phase motor using microcontroller and bluetooth module HC-05.

II. MATERIAL AND METHODS

A. Modelling of Single phase Induction motor Based on Double Field Revolving Theory

The double field revolving theory can be effectively used to obtain equivalent circuit of a single phase IM. This method consists of determining the parameters of both the field at any given slip. When the two fields are known, the torque produced by each can be obtained. The difference between these two torques is the net torque acting on the rotor [2]. The equivalent circuit of single phase IM in S-domain is shown in figure.

Where,

R_1-Stator main winding resistance (Ω)

L_1-Stator main winding inductance (H)

R_2-Rotor winding resistance (Ω)

L_2-Rotor winding reactance (Ω)

R_4-Core loss equivalent resistance (Ω)

[1]*Associate Professor, Department of EEE, Sri Sivasubramaniya Nadar College of Engineering, Kalavakkam, Chennai, Tamilnadu, India. deepalaxmir@ssn.edu.in

[2] Professor, School of Electrical Engineering (SELECT), Vellore Institute of Technology, Chennai, Tamilnadu, India. vaithilingam.c@vit.ac.in

X_m- Magnetising reactance (Ω)

$\check{s}$- Slip

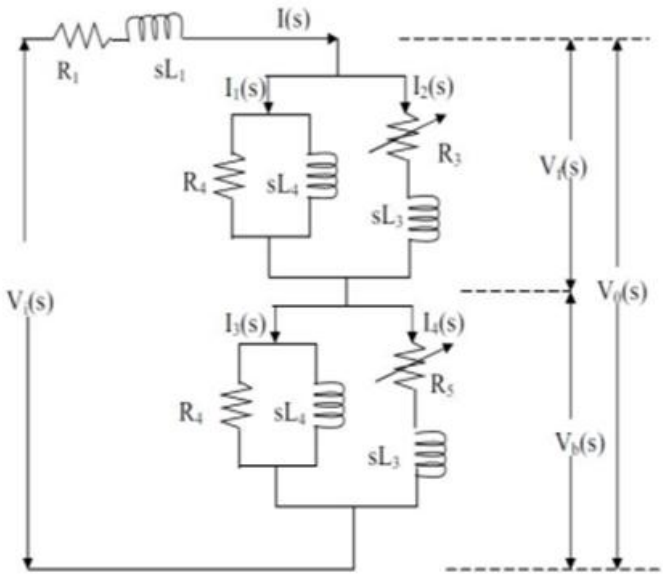

Fig. 1. Equivalent circuit of single-phase induction motor in S domain

$$R_3 = \frac{r_2}{\check{s}} = \frac{R_2}{2\check{s}}$$

$$R_5 = \frac{r_2}{\check{s}} = \frac{R_2}{2(2-\check{s})}$$

$$X_3 = X_2/2$$

$$X_4 = X_m/2$$

The basic equations, which govern the model of the induction motor, can be derived from the equivalent circuit.

Current flowing through the stator is expressed as

$$I(s) = \frac{(V_i(s) - V_o(s))}{(R_1 + sL_1)} \qquad (1)$$

Model for Forward Field

Current flowing through the stator can be expressed as

$$I(s) = I_1(s) + I_2(s) \qquad (2)$$

If the rotor current referred to the stator is taken as I_2, then the iron loss and magnetising component of the no-load current can be expressed as

$$I_1(s) = I(s) - I_2(s) \qquad (3)$$

The forward field voltage can be obtained from the expression

$$V_f(s) = V_o(s) - V_b(s) = I_1(s) * \left\{ {}^{sR_4L_4}/_{(R_4 + sL_4)} \right\} \qquad (4)$$

Voltage across the rotor inductance is expressed as

$$V_f(s) - I_2(s) * \left(\frac{R_2}{2\check{s}}\right) \quad (5)$$

Rotor current referred to the stator can be expressed as

$$I_2(s) = \frac{\left(V_f(s) - V_1(s)\right)}{sL_3} \quad (6)$$

Where,

$$V_1(s) = I_2(s) * R_3 \quad (7)$$

Airgap power developed by the motor is given by the expression,

$$P_{gf}(s) = I_2(s)^2 * \frac{R_2}{2\check{s}} \quad (8)$$

Model for Backward Field

Current flowing through the stator can be expressed as

$$I(s) = I_3(s) + I_4(s) \quad (9)$$

If the rotor current referred to the stator is taken as I_4, then the iron loss and magnetising component of the no-load current can be expressed as

$$I_3(s) = I(s) - I_4(s) \quad (10)$$

The backward field voltage can be obtained from the expression

$$V_b(s) = V_o(s) - V_f(s) = I_3(s) * \left\{{}^{sR_4L_4}/_{(R_4 + sL_4)}\right\} \quad (11)$$

Voltage across the rotor inductance is expressed as

$$V_b(s) - I_4(s) * \left(\frac{R_2}{2(2 - \check{s})}\right) \quad (12)$$

Rotor current referred to the stator can be expressed as

$$I_4(s) = \frac{(V_b(s) - V_2(s))}{sL_3} \quad (13)$$

Where,

$$V_2(s) = I_4(s) * R_5 \quad (14)$$

Airgap power developed by the motor is given by the expression,

$$P_{gb}(s) = I_4(s)^2 * \frac{R_2}{2(2 - \check{s})} \quad (15)$$

Torque developed by the motor is given by the expression

$$T(s) = \frac{\left(P_{gf}(s) - P_{gb}(s)\right)}{2\pi n_s} \quad (16)$$

The load balance equation is given by

$$\omega(s) = \frac{\left(T(s) - T_L(s)\right)}{Js + B} \quad (17)$$

By using the Equations (1) to (17), the simulink model of the single phase IM can be obtained as shown in figure 2. The simulink model is reduced to obtain the transfer function of single phase IM using MATLAB functions.

$$\frac{\theta(s)}{V_i(s)} = \left\{\frac{R_1R_4(R_3-R_5)/(2\pi n_s)}{s^2(JR_1R_4+L_3L_4R_4^2(R_3-R_5)+BL_1R_4)+s(BR_1R_4+R_1R_3R_4(L_4+L_3))+R_1(R_3-R_5)}\right\} \quad (18)$$

Equation (18) represents the transfer function of the IM. Substitute the values of the parameters from table 1 in equation (18).

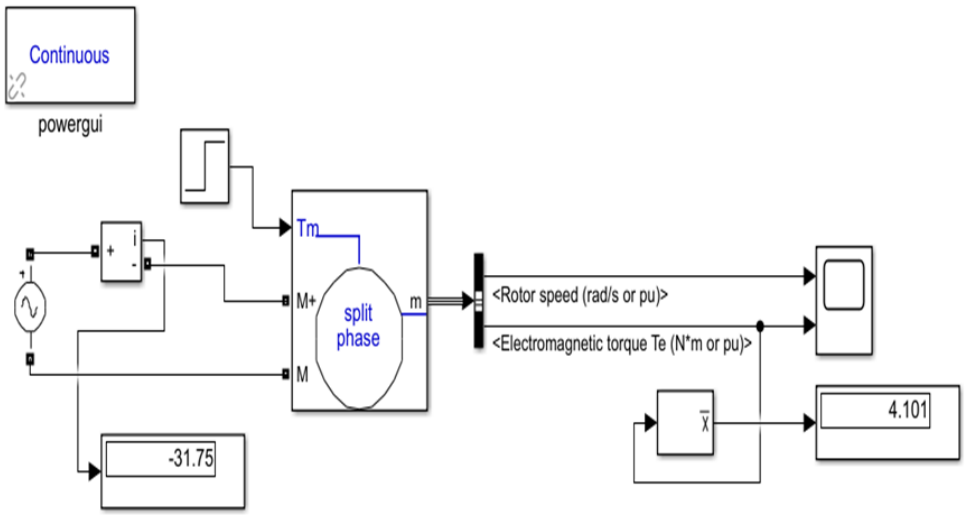

Fig. 2. Simulink Model of single-phase IM

TABLE 1. Modelling parameters for single phase IM

Parameters	Values	Parameters	Values
Rs(ohm)	2.02	LlS(H)	8.50E-03
Lls(H)	7.40E-03	Pole pairs	2
Rr'(ohm)	4.12	J(kg.m^2)	0.0146
Llr(H)	5.60E-03	B(N.m.s)	0
Lms(H)	0.1772	Frequency(Hz)	50
RS(ohm)	7.14	Turns ratio	1.18
Rst(ohm)	2	Rru(ohm)	18
Cs(farad)	2.55E-04	Cru(farad)	2.11E-05

$$\frac{\theta(s)}{V_i(s)} = \frac{0.2054}{s^2+3.02s+0.129} \quad (19)$$

From state space analysis, =AX+BU

[A]-System matrix (nxn)

[B]-control matrix (nxm)

[X]-State matrix (nx1)

[U]-Input matrix (nxm)

Where n-number of states ; m-number of inputs

$$\ddot{\theta} + 3.02\dot{\theta} + 0.129\theta = 0.2054V_i$$

The state variables are $\dot{X}_1 = \dot{\theta}$ and $\dot{X}_2 = \ddot{\theta} = -3.02\dot{\theta} - 0.129\theta + 0.2054V_i$. Equation (20) represents the state equation of IM.

$$\begin{pmatrix} \dot{X}_1 \\ \dot{X}_2 \end{pmatrix} = \begin{bmatrix} 0 & 1 \\ -0.129 & -3.02 \end{bmatrix} \begin{pmatrix} X_1 \\ X_2 \end{pmatrix} + \begin{pmatrix} 0 \\ 0.2054 \end{pmatrix} (V_i) \qquad (20)$$

$\dot{X}$=AX+BU where U=-Kx (control law)

$\dot{X}$=AX+B(-Kx)

$\dot{X}$=(A-BK)X

$\dot{X}$=$\hat{A}$X

Where,

$$\hat{A} = \begin{bmatrix} 0 & 1 \\ -0.129 - 0.2054K_1 & -3.02 - 0.2054K_2 \end{bmatrix}$$

$$\left|SI - \hat{A}\right| = s^2 + s(3.02 + 0.2054K_2) + (0.129 + 0.2054K_1) \quad (21)$$

Figure 3 shows the MATLAB command window with the transfer function after substituting the values from Table1.

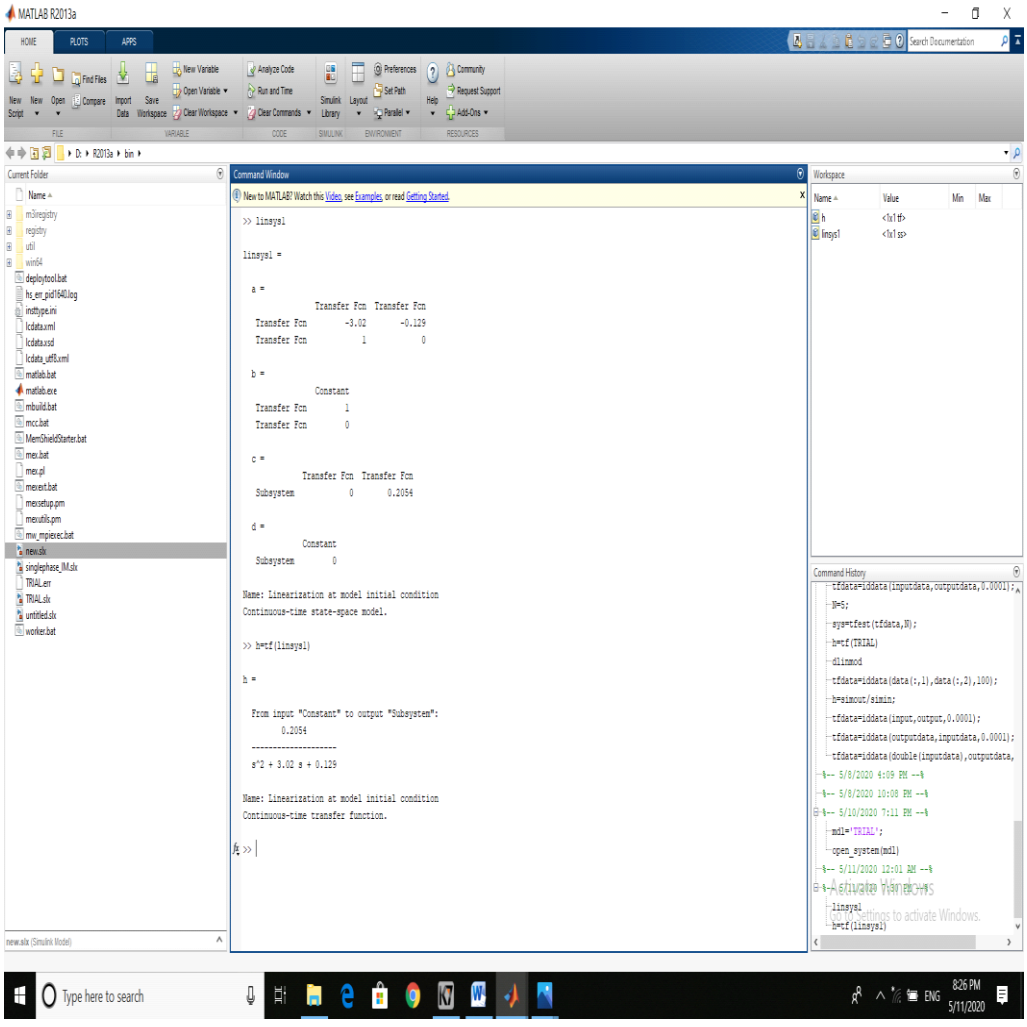

Fig. 3. Transfer function of the IM in command window

2.2 *PID Tuning by pole placement technique for over damped system*

2.2.1 PID Controller:

A proportional–integral–derivative (PID) controller has a control loop feedback. The controller, continuously calculates an error value, e(t). The error is the difference between a desired set point SP = r(t), measured process variable PV = y(t), and applies a correction based on proportional, integral, and derivative terms. The controller attempts to minimize the error over time by adjustment of a control variable u(t), determined by a weighted sum of the control terms. The overall control function can be expressed mathematically as,

$u(t) = Kpe(t) + Ki \int e(t)dt + Kd\, e(t)$

Where, u(t) is the output of the controller and Kp, Ki and Kd are coefficients for proportional, integral and derivative terms respectively

The term P is proportional to the current value of the error, e(t) and term I accounts for past values of the error and integrates them over time to produce I term. The integral term seeks to eliminate the residual error by adding a control effect due to the historic cumulative value of the error. The term D is the estimate of future trend of the error, based on its current rate of change. It may reduce the effect of the error by exerting a control influence generated by the rate of error change. The more rapid the change, the greater the controlling or dampening effect.

2.2.2 Characteristics of PID Controller

The **proportional controller** is effective on the errors since its output is directly proportional to the error. But the proportional controller has a disadvantage of steady state error. The output will not settle at the set point. It will have error. The **derivative controller** provides smoother response, the system will be having no oscillations. The output of the derivative controller is the function of the change in error. The damping factor decides the transient response of the system. This reduces the peak overshoot problem of the system. The **integral controller** is used to eliminate the steady state error. The output of the integral controller is the function of the accumulated error. The past errors are summed and the integral controller will create output proportional to the accumulated error.

settling time=1/dominant pole

$$t_s = 1 \text{ sec}$$

Assumption of poles:P_1=-1,$P_2 = -4$

1/(s+1)(s+4)=1/($s^2 + 5s + 4$)

The characteristic equation of above transfer equation is

$s^2 + 5s + 4$ (22)

On comparing the coefficients of (21) and (22), the gains of the PID controller are obtained

$K_1 = 18.8 = K_P$

$K_2 = 9.6 = K_D$

The value of K_D was chosen based on trial and error method until the required response was arrived.

$K_I = 0.00127$

The characteristics of PID controller is represented in table 2.

TABLE 2. Characteristics of PID controller

Term	**Rise time**	**Overshoot**	**Settling time**	**Steady state error**
K_p	Decrease	Increase	Minor change	Decrease

K_i	Decrease	Increase	Increase	Eliminate
K_d	Minor change	Decrease	Decrease	No change

III. RESULTS AND DISCUSSION

3.1 MATLAB Simulation

Matlab simulation for the designed IM with tuned PID in closed loop is done for three different voltage conditions: rated voltage (230V), under voltage (190V), over voltage (240V). AC voltage regulator is simulated by connecting back to back SCRs. The error is obtained by comparing the actual speed and the reference speed is converted into angular position using the integrator and given as input to the PID. The output of the PID is used to produce PWM pulses, which are given as gating pulses to the SCRs. The figures 4 and 5 show simulink model for the rated voltage (230 V) and speed and electromagnetic torque waveforms for rated voltage condition. The figures 6 and 7 show simulink model for the under voltage (190 V) and speed and electromagnetic torque waveforms for under voltage condition. The figures 8 and 9 show simulink model for the over voltage (240 V) and speed and electromagnetic torque waveforms for over voltage condition.

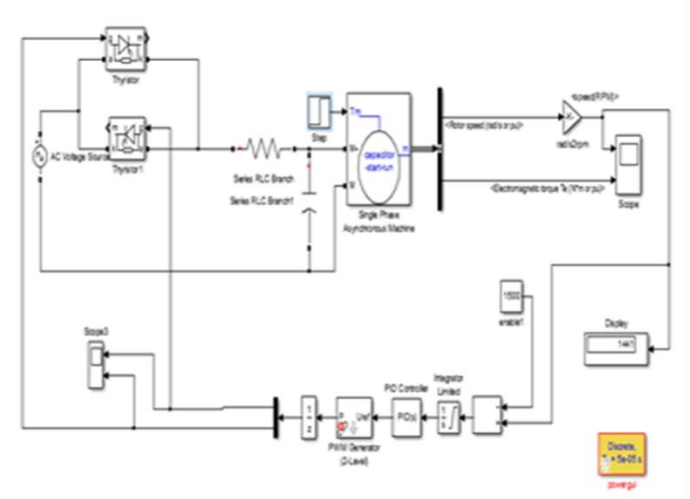

Fig. 4. Simulink model for the rated voltage (230 V)

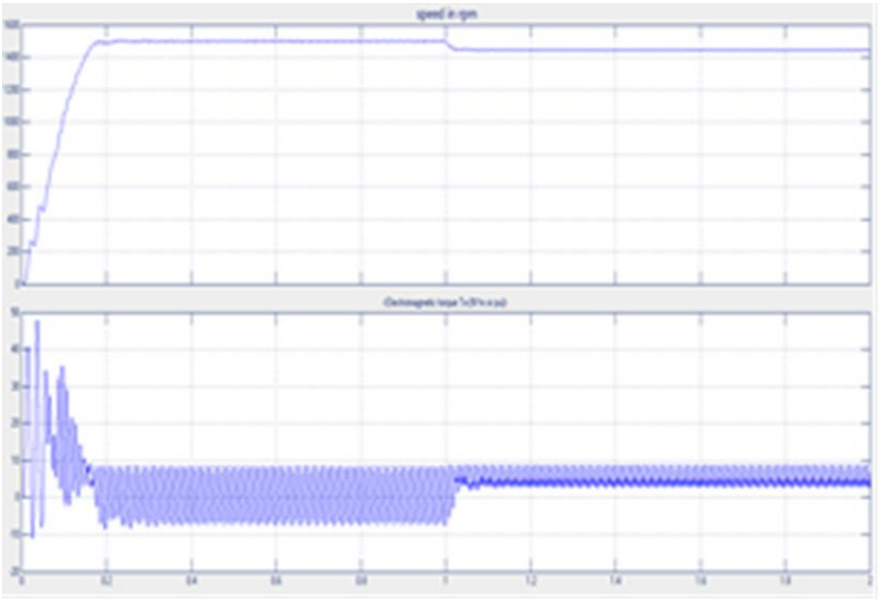

Fig. 5. Speed and electromagnetic torque waveforms for rated voltage condition

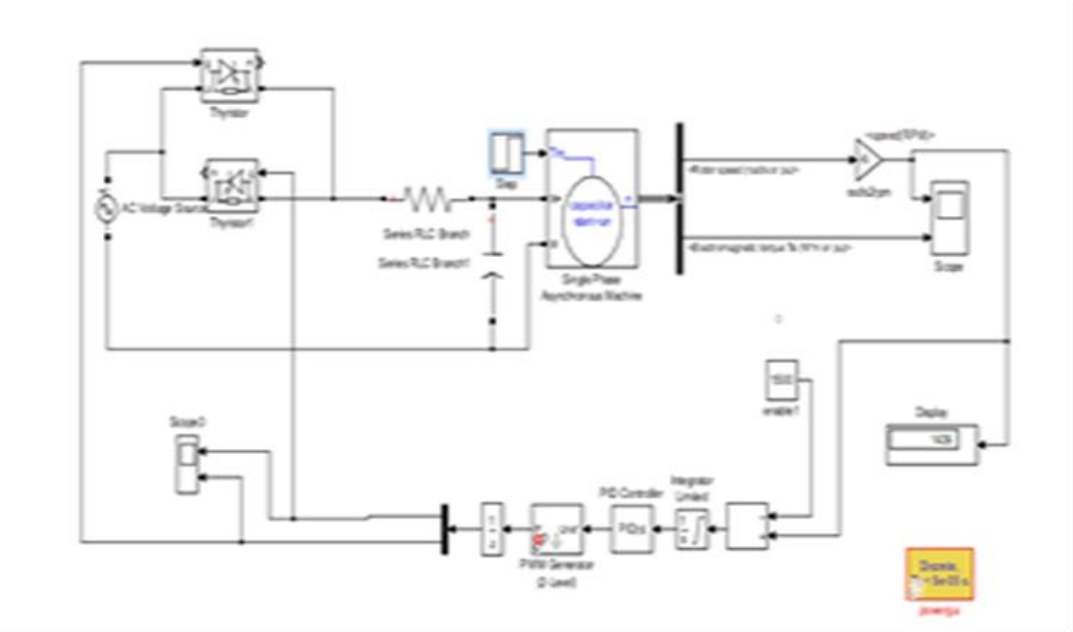

Fig. 6. Simulink model for the under voltage (190 V)

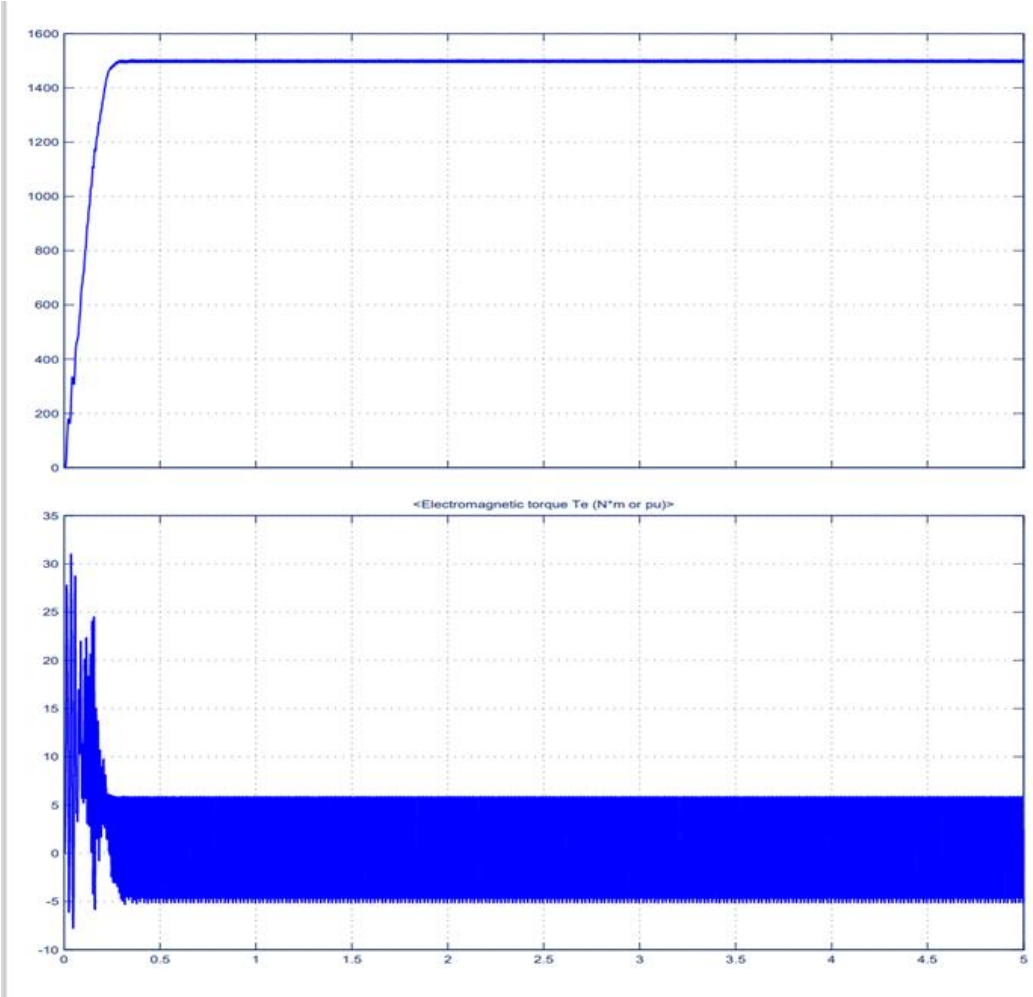

Fig. 7. Speed and electromagnetic torque waveforms for under voltage condition

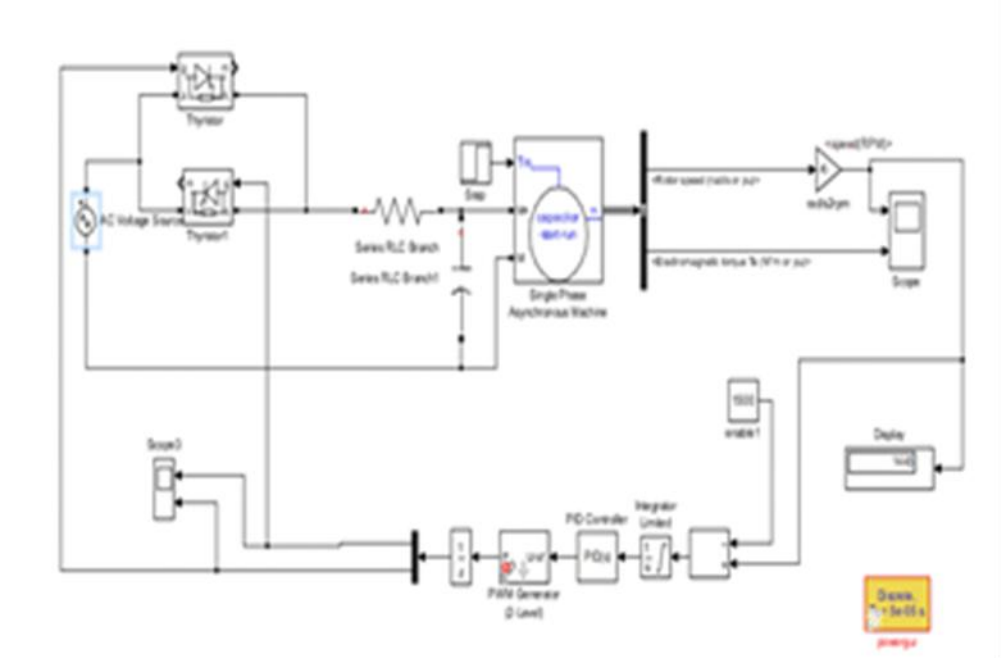

Fig. 8. Simulink model for the over voltage (240 V)

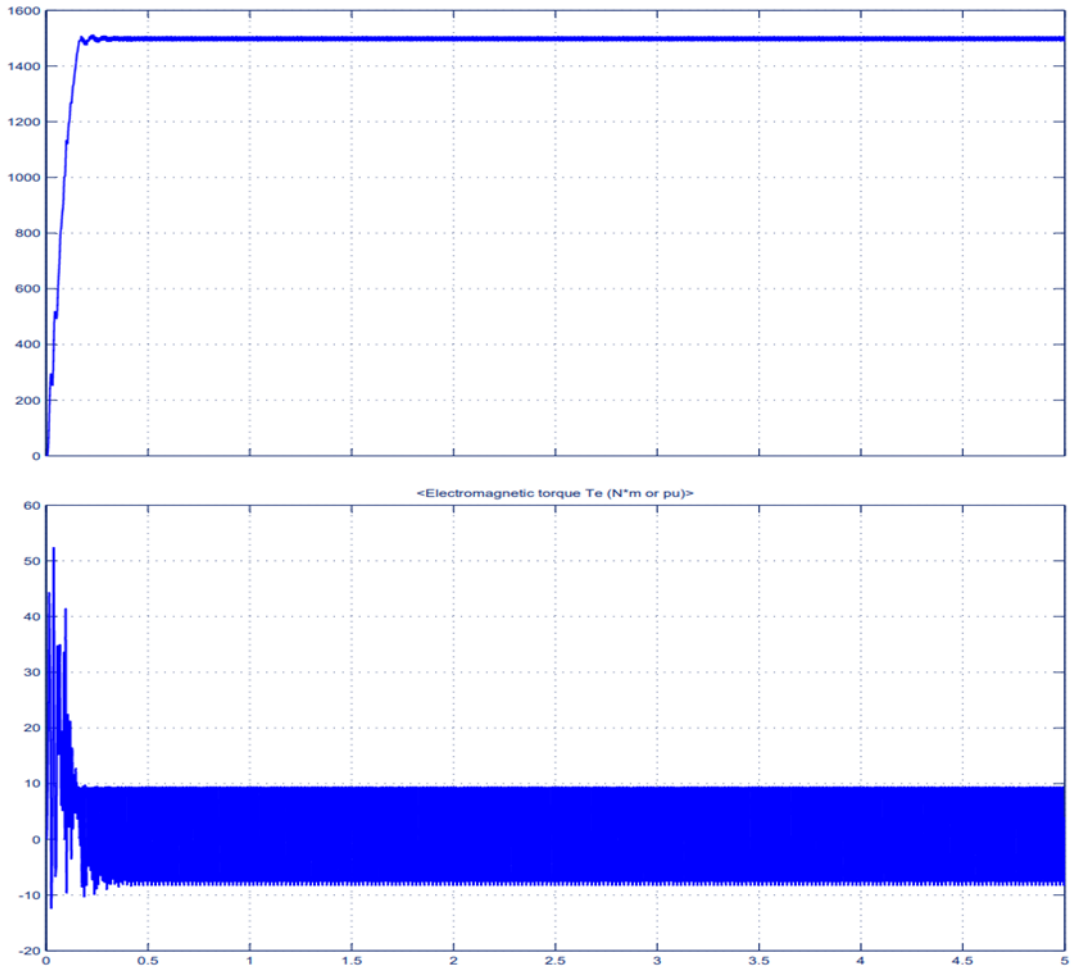

Fig. 9. Speed and electromagnetic torque waveforms for over voltage condition

Due to the PID controller in the closed loop, the speed value gets saturated at the reference speed irrespective of the input voltage given. The response is smoother without having any overshoot. The comparison between the open loop and closed loop performance of single phase induction motor has been made. It is inferred that electromagnetic torque has been increased due to the inclusion of PID controller with K_p=18.8; Ki= 0.00127, K_d=9.6 in the feedback loop. Also reduction in setting time has been observed. The torque increased from 4 N-m to 9 N-m ,from 2.5 N-m to 5 N-m and from 5 N-m to 10 N-m for 230V ,190V and 240V respectively.

3.2 Hardware Implementation of Microcontroller Based Condition monitoring of single phase induction motor

3.2.1 ARDUINO

Arduino is an open-source based on a hardware and software. It's a microcontroller based on the Atmel ATmega328 which can operate at 5V. The microcontroller can be programmed easily by connecting it to a computer via USB cable and using Arduino software (IDE) which is built based on Java. This board offers digital and analog inputs and outputs as well as PWM output [3-6]. The ARDUINO UNO specifications are represented in table 3. The table 4 provides details about the pins of Arduino UNO used in the research.

TABLE 3. ARDUINO UNO specifications

Microcontroller	**ATmega328**
Architecture	AVR
Flash Memory	32 KB
SRAM	2 KB
Clock Speed	16 MHz
No of PWM output ports	6
Power consumption	5V

TABLE 4. Arduino Pins used in the research

ARDUINO pin number	**Connected to**
D0	Bluetooth Rx Pin
D1	Bluetooth Tx Pin
D2	4n35 5th Pin
D3	Speed D0 Pin
D4	LCD 13th Pin
D5	LCD 12th Pin
D6	LCD 11th Pin
D7	Switch
D8	LCD 14th Pin
D9	Cooling Fan
D10	MOC3021 1st Pin
D11	Relay
D12	LCD 6th Pin

D13	LCD 4th Pin
A0	LM35
A1	Current Sensor
A2	Buzzer

3.2.2 TRIAC (BT136)

A bidirectional triode thyristor is a three terminal electronic component that conducts current in either direction when triggered. Applying a trigger at a controlled phase angle of the AC in the main circuit allows control of the average current flowing into a load (phase control). This is commonly used for controlling the speed of a universal motor, dimming lamps, and controlling electric heaters. Table 5 provides information about the specifications of BT 136.

TABLE 5. BT136 specifications

Parameter	**Value**
Maximum terminal current	4A
On-state gate voltage	1.4V
Gate trigger current	10mA
Maximum terminal voltage	600V
Holding current	2.2mA
Latching current	4mA

3.2.3 Induction motor

Induction motor or asynchronous motor is widely used in industries because of its reliability, high efficiency low cost and good self-starting capability. The specifications of the induction motor used in the project are represented in table 6.

TABLE 6. Induction motor specifications

Parameters	Values
Voltage	220-240V
Frequency	50Hz
Power	40W
Current	0.4A
Number of poles	4

3.2.4 Opto coupler (4n35 and MOC3021)

An optocoupler, is an electronic component that interconnects two separate electrical circuits by means of a light sensitive optical interface. The emitter of always an LED, and the light sensitive device is phototransistor and DIAC for 4 n35 and MOC3021 respectively. The figure 10 (a) and 10 (b) show the opto-couplers 4n35 and MOC3021 respectively.

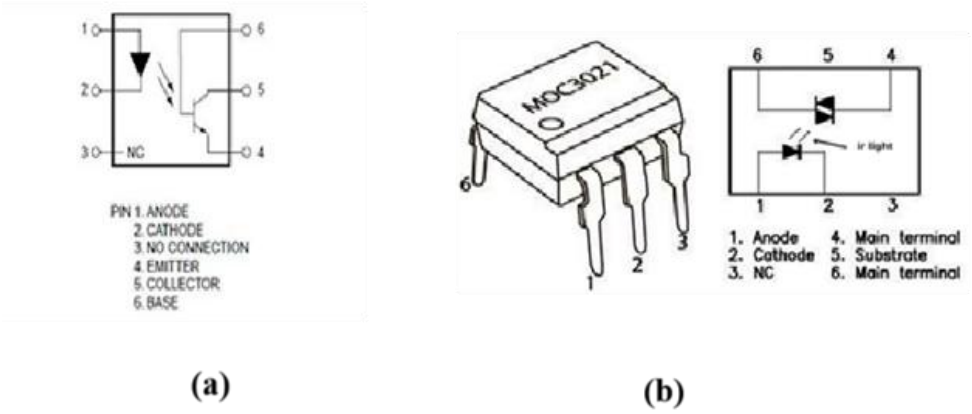

Fig. 10. Opto-couplers (a) 4n35 and (b) MOC3021

3.2.5 Speed sensor (LM393)

To measure speed of a motor using Arduino, LM393 speed sensor is used which is shown in figure 11. The LM393 speed sensor module is an infrared light sensor integrated with LM393 voltage comparator IC. The sensor part of the LM393 speed sensor module consists of an Infrared LED and an NPN photo transistor. These two components are placed facing each other is a special housing made of black thermoplastic. This special housing ensures that the photo transistor receives light only from the Infrared LED. Coming to control unit, it is made up of LM393 Voltage Comparator and a few passive electronic components. The signal from the photo transistor is given to the LM393 and based on the presence or absence of an object between the Infrared LED and the Photo Transistor, the output of the LM393 IC will either be HIGH or LOW.

Mount the encoder wheel on the top such that the wheel passes through the gap provided in the housing of the sensor(i.e. between the Infrared LED and NPN photo transistor). Since the wheel is fixed to the motor, one rotation of the motor implies one rotation of the wheel. The encoder wheel consists of 3 poles. Determining the rotational speed of a rotating object. Whenever the infrared light is obstructed for 3 times from falling on the photo transistor, the wheel makes one rotation.

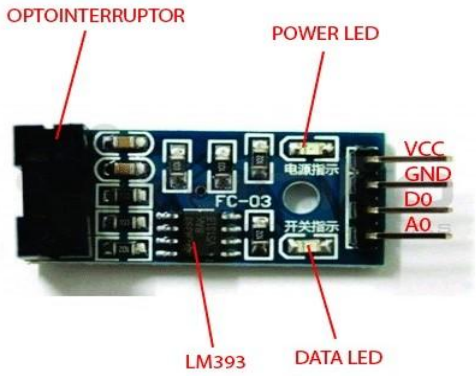

Fig. 11. Speed Sensor (LM393)

3.2.6 Temperature Sensor (LM35)

LM35 is a temperature sensor, whose output voltage varies, based on the temperature around it. It is a small and cheap IC which can be used to measure temperature anywhere between -55°C to 150°C. It can easily be interfaced with any microcontroller that has ADC function or any development platform like Arduino. Power the

IC by applying a regulated voltage like +5V (V_S) to the input pin and connect the ground pin to the ground of the circuit. The second pin gives analog output of 10mV/°C. The figure 12 shows the temperature sensor (LM 35).

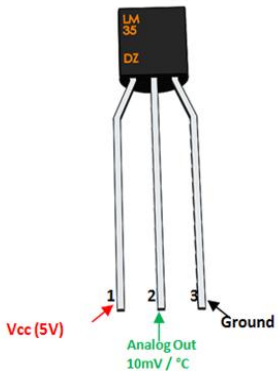

Fig. 12. Temperature Sensor (LM35)

3.2.7 Current Sensor (ACS712)

ACS712 current sensor is used to measure and calculate the amount of current applied to the conductor without affecting the performance of the system. It is a fully integrated, hall-effect based linear sensor IC. It has 2.1kV RMS voltage isolation along with a low resistance current conductor. Current sensor detects the current in a wire or conductor and generates a signal proportional to the detected current either in the form of analog voltage or digital output. There is a copper strip connecting the IP+ and IP- pins internally. When some current flows through this copper conductor, a magnetic field is generated, which is sensed by the hall effect sensor. The hall effect sensor then converts this magnetic field into appropriate voltage. In this method, the input and the output are completely isolated. The figure 13 depicts the current sensor (ACS 712).

Fig. 13. Current Sensor (ACS 712)

3.2.8 Relay

A relay is a type of a switch that acts as an interface between microcontrollers and AC Loads. Relay disconnects the load from the supply when abnormalities are detected. The figure 14 shows the 5 V relay module.

Fig. 14. 5V Relay Module

3.2.9 Bluetooth module

Bluetooth communication is a 2.4GHz frequency based RF Communication with a range of approximately 10 meters. It is a frequently used low range communication for data transfer, audio systems, hands free, computer peripherals. Pair the bluetooth module with an Android Phone, send data from Android Phone to the bluetooth module using a simple App, read the data from bluetooth module through Arduino and finally, display the data and control a device based on the data. The figure 15 shows topview and bottom view of HC-05 bluetooth module.

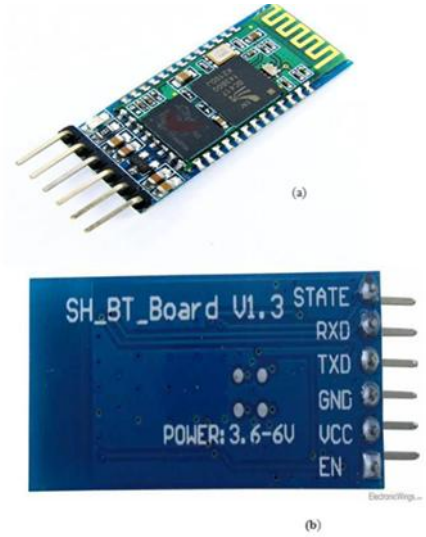

Fig. 15. HC-05 Bluetooth module (a) Bottom view and (b)Top view

HC-05 is a Bluetooth module which is designed for wireless communication. This module can be used in a master or slave configuration. Bluetooth serial modules allow all serial enabled devices to communicate with each other using Bluetooth.

Pin configuration:

1. **Key/EN:** It is used to bring Bluetooth module in AT commands mode. If Key/EN pin is set to high, then this module will work in command mode. Otherwise by default it is in data mode. The default baud rate of HC-05 in command mode is 38400bps and 9600 in data mode.

HC-05 module has two modes,

1. **Data mode:** Exchange of data between devices.
2. **Command mode:** It uses AT commands which are used to change setting of HC-05. To send these commands to module serial (USART) port is used.

2. **VCC:** Connect 5 V or 3.3 V to this Pin.
3. **GND:** Ground Pin of module.
4. **TXD:** Transmit Serial data (wirelessly received data by Bluetooth module transmitted out serially on TXD pin)
5. **RXD:** Receive data serially (received data will be transmitted wirelessly by Bluetooth module).
6. **State:** It tells whether module is connected or not.

3.2.10 LCD

The figure 16 depicts LCD module. 16x2 indicates that it can display 32 characters in 2 lines. It has 16 pins. It is used as display unit.

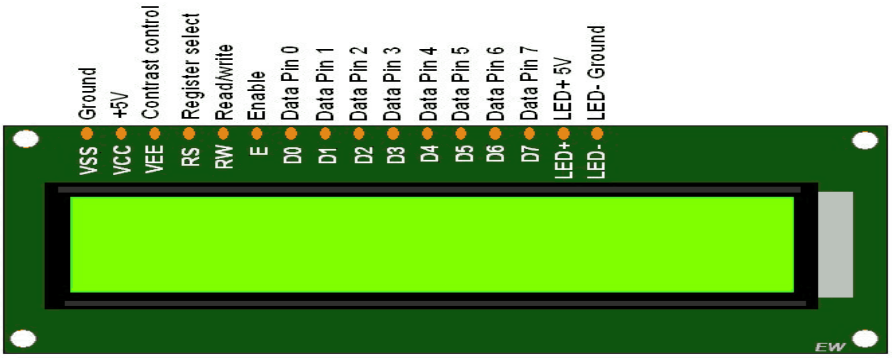

Fig. 16. LCD Module

3.2.11 Circuit diagram and PCB

The overall circuit layout is divided into speed control, monitoring and protection scheme. The speed control scheme involves zero crossing detector circuit, arduino and gating pulse generation circuit for TRIAC for ac voltage control.

3.2.12 Zero crossing detector circuit

The circuit diagram of ZCD and PCB layout of gate pulse generation circuit are shown in figures 17 and 18.

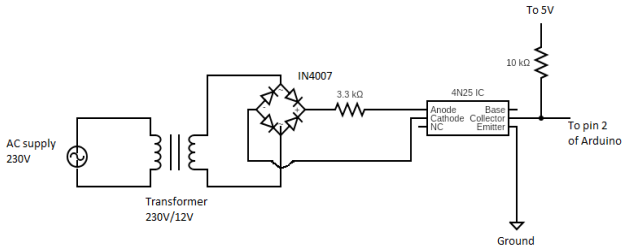

Fig. 17. Circuit diagram of ZCD

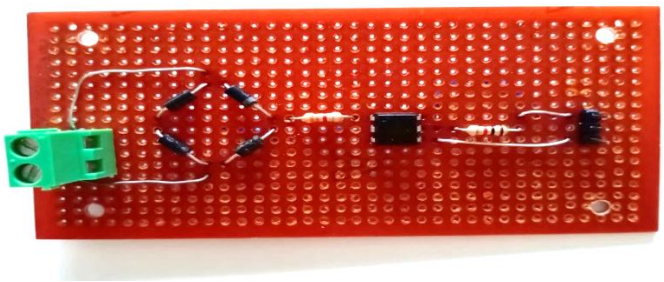

Fig. 18. PCB layout of ZCD

AC motor driver circuit uses zero crossing detector which employs optoisolator 4n35. First the AC voltage from the main supply is stepped down using a transformer to 12V. The stepped down AC voltage is fed to the full bridge rectifier circuit built using 1N4007 diodes. The rectified voltage is supplied to pins 1 and 2 of 4n35 optocoupler. The 4n35 is a phototransistor type optocoupler. At the instant of zero crossing, pulses are generated as shown in figure 19.

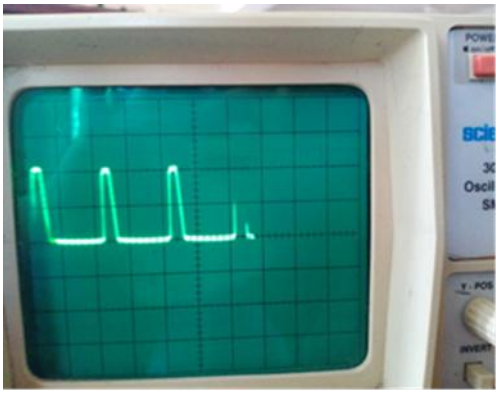

Fig. 19. Output pulses of ZCD

The input to arduino is the pulses generated by the zero crossing circuit. Depending upon the required speed, delay is calculated. With zero crossing as the reference, after the calculated delay, the interrupt routine shoots a HIGH pulse for 50 microseconds after the delay and is activated at pin 10 of the Arduino.

3.2.13 AC Voltage Control Using TRIAC (BT136)

The circuit diagram and PCB layout of gate pulse generation circuit are shown in figures 20 and 21.

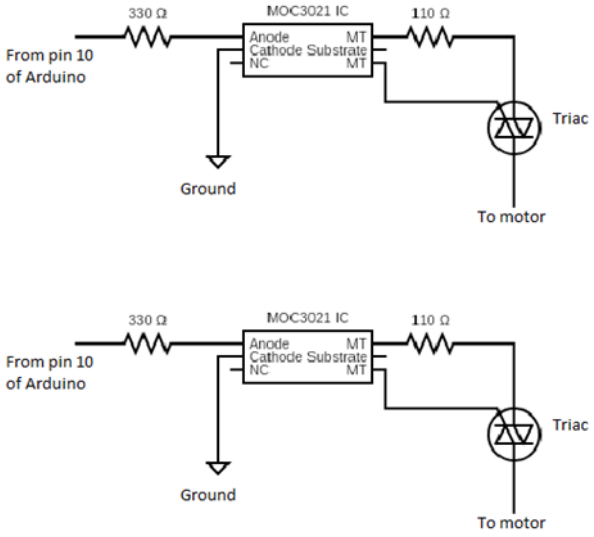

Fig. 20. Circuit diagram of gate pulse generation circuit

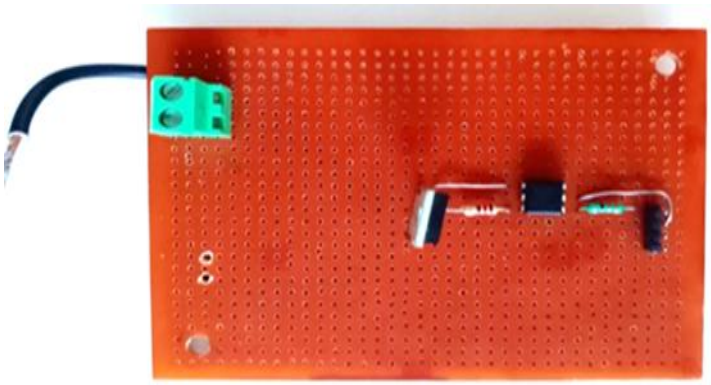

Fig. 21. PCB layout of gate pulse generation circuit

The pin 2 of MOC3021 is connected to ground and pin 1 is connected to pin 10 of the Arduino to receive the pulses. The Main Terminal pins of photo-TRIAC(MOC3021) , pins 4 and 6 are connected to pins 3 (Base) and 2 (Main Terminal 2) of BT136 to provide the gating signal.

3.2.14 Monitoring and Protection Scheme

The monitoring and protection scheme involves temperature sensing, speed sensing and bluetooth circuits. The figure 22 shows PCB layout of temperature sensor. The temperature sensor LM35 data pin is connected to the analog pin of arduino. The analog data is converted into temperature after calculations and is displayed in the LCD, serial monitor and the APP. The speed sensor LM393 produces pulses when the encoder wheel passes through it. The pulse is converted into RPM with the help of arduino. More the spikes in the encoder wheel higher the resolution and the speed will be accurate. The encoder wheel designed for the motor used has 3 spikes. The figure 23 depict the speed sensing circuit.

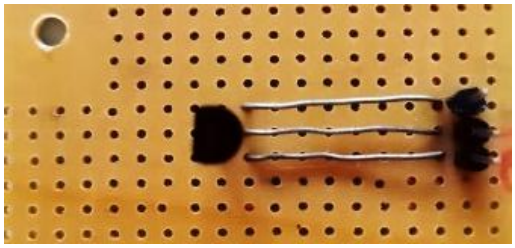

Fig. 22. PCB layout of Temperature Sensor

The current sensor ACS712 is used to measure the current flow in the circuit. The necessary conversions are done through the Arduino code and are displayed in the LCD display and App. The relay protects the induction motor by making and braking the circuit. The relay is controlled through the app and the temperature conditions. When the temperature exceeds the threshold, the relay breaks the circuit and the cooling fan switches on with a buzzer sound. The rise in temperature is due to increase in I^2R losses. Hence current sensor along with temperature sensor have been used. The current sensor has been used as a predictive device.

Fig. 23. Speed Sensing circuit

.

3.2.15 Bluetooth Circuit

The figure 24 (a) and (b) depict the HC-05 connected to ARDUINO UNO and Android APP development using MIT APP INVENTOR respectively. Using Bluetooth module HC-05 the data transmission and reception between the ardunio and the android app takes place. The android application CONDITION MONITORING is developed using MIT app inventor. The app displays the real time data of the sensors connected in the monitoring circuit and

helps in maintenance of the plant. The code blocks of the developed APP (Left), Front-end of the CONDITION MONITRING APP (Right) are shown in figure 25. The figure 26 shows the overall layout of IM control, monitoring and protection.

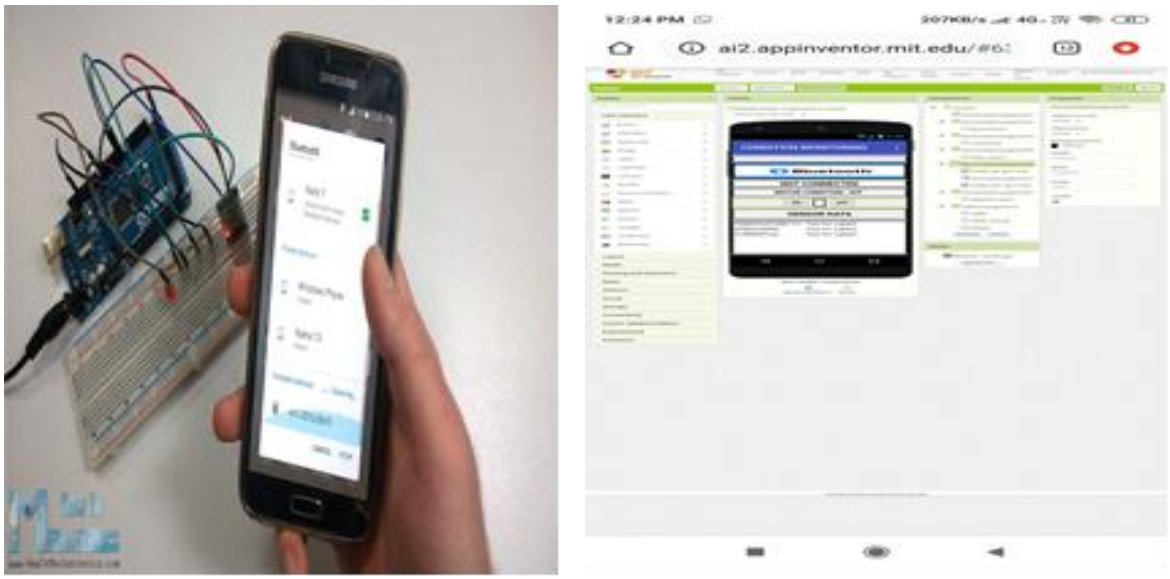

Fig. 24. (a) HC-05 connected to ARDUINO UNO and (b) Android APP development using MIT APP INVENTOR

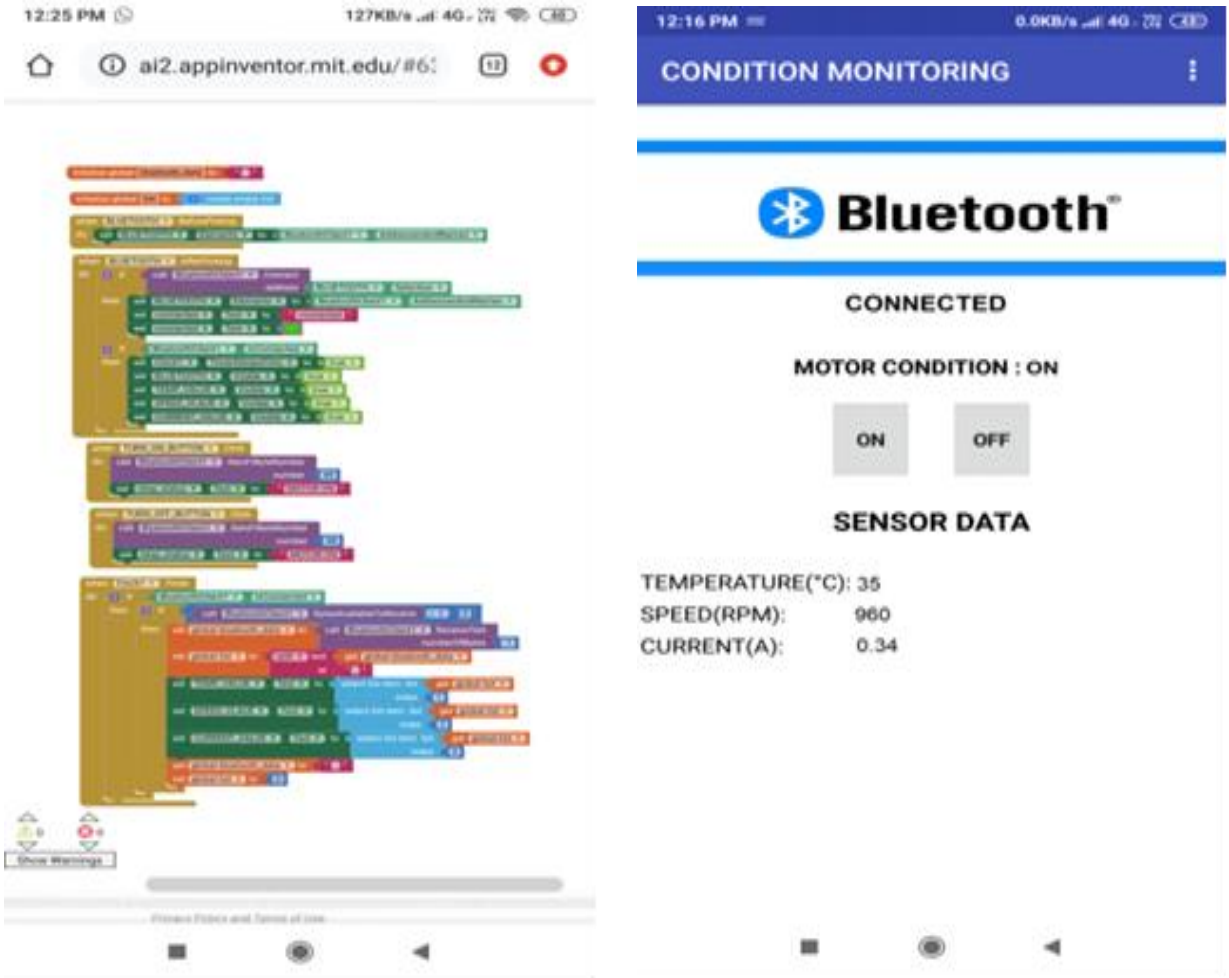

Fig. 25. Code Blocks of the developed APP (Left), Front-end of the condition monitoring APP (Right)

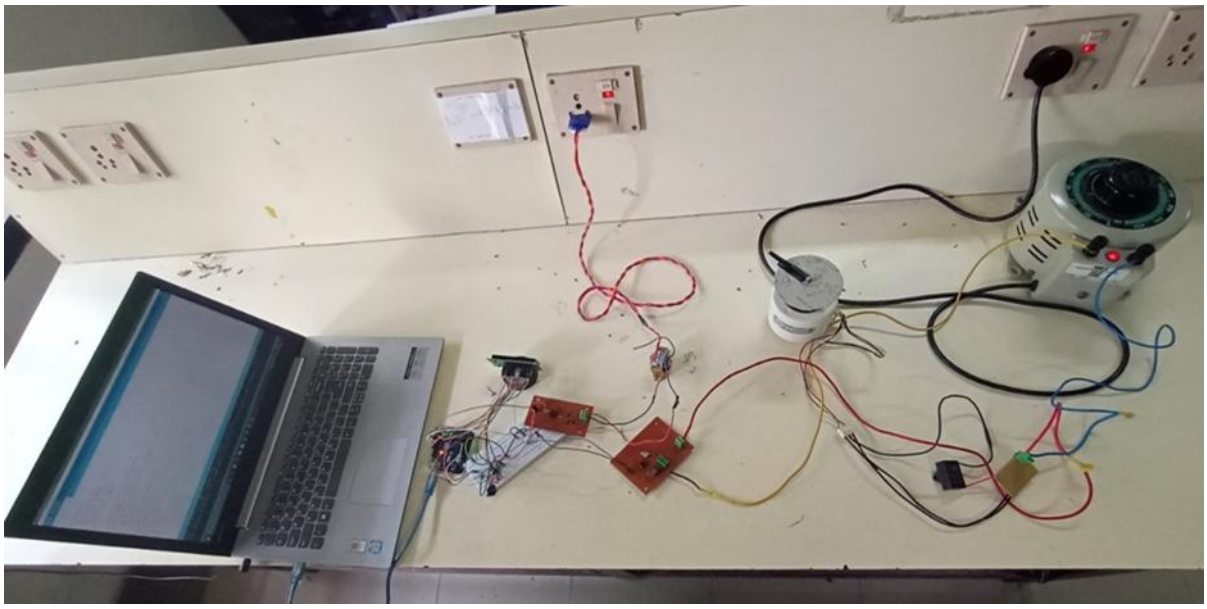

Fig. 26. Overall layout

IV CONCLUSION

The PID controller had been designed based on pole placement technique. Closed loop speed control of 1 phase induction motor had been simulated using MATLAB SIMULINK for various conditions (rated voltage, under voltage and over voltage). The results were studied. PCB design of zero crossing detector, gate pulse generation circuit, speed, current and temperature sensors have been done. Using LM35, LM393 and ACS712 sensors, the temperature, speed and current are sensed and displayed respectively. The data transmission and reception

between the Ardunio and the android app has been obtained using bluetooth module HC-05. The android application condition monitoring had been developed using MIT app inventor. The app displayed the real time data of the sensors connected in the monitoring circuit and helps in maintenance of the plant.

REFERENCES

[1] B. S Cunha, "Single-Phase Induction Motor Speed Control Through a PIC Controlled Sinusoidal PWM Inverter," *Master's Dissertation*, UFU, School of Electrical Engineering, Uberlândia, MG, Brazil, 2000.

[2] A. Diaz, R. Saltares., C. Rodriguez, R. F., Nunez, E. I., Ortiz-Rivera, J., and Gonzalez-Llorente., " Induction motor equivalent circuit for dynamic simulation," [Electric Machines and Drives Conference 2009.IEMDC '09. IEEE International, pp. 858-863,2009.

[3] Manish Paul ,Antara Chaudhury , SnigdhaSaikia, "Hardware Implementation of Overvoltage and Under voltage Protection," International Journal of Innovative Research in Electrical , Electronics, Instrumentation and Control Engineering, vol. 3, Issue. 6, 2015.

[4] S, Nicklesh , S. PalaniKumar , M. Priya , "Design and Implementation of Microcontroller Based Motor Controller with Temperature Sensor," International Journal for Research in Applied Science & Engineering Technology (IJRASET), vol.4, Issue. VII, ISSN: 2321-9653, 2016.

[5] Rupali M, Shivpuje.,Swapnil D, Patil, "Microcontroller Based Fault Detection and Protection System for Induction Motor," [International Conference on Intelligent Computing and Control Systems ICICCS 2017.

[6] Kpochi Paul Kpochi ., Eiyike Jeffrey Smith ., and Abubakar Attai Ibrahim, " Microcontroller-based under and over voltage protection device," American Journal of Engineering Research (AJER), vol. 7, Issue. 8,pp.16-20,2018.